

# DEUTSCHES ELEKTRONEN-SYNCHROTRON DESY

DESY 79/87  
December 1979



## ANGULAR ASYMMETRIES OF $e^+e^-$ ANNIHILATION TO THREE JETS

by

K. Kolfer

*Sektion Physik, Universität München*

H. G. Sander

*Physikalisches Institut, TH Aachen*

T. F. Walsh

*Deutsches Elektronen-Synchrotron DESY, Hamburg*

P. M. Zerwas

*Institut für Theoretische Physik, TH Aachen  
and  
Deutsches Elektronen-Synchrotron DESY, Hamburg*

NOTKESTRASSE 85 · 2 HAMBURG 52

To be sure that your preprints are promptly included in the  
HIGH ENERGY PHYSICS INDEX ,  
send them to the following address ( if possible by air mail ) :

DESY  
Bibliothek  
Notkestrasse 85  
2 Hamburg 52  
Germany

DESY 79/87  
December 1979

Abstract

We discuss the angular asymmetries of 3-jet events in  $e^+e^-$  annihilation, originating from hard gluon bremsstrahlung off quarks. Lepton beam polarization helps to disentangle the various helicity components of the bremsstrahlung cross section. They are sensitive to the spin of the radiated quantum but are otherwise parameter-free.

Angular Asymmetries of  $e^+e^-$  Annihilation to Three Jets

by

K. Koller  
Sektion Physik, Universität München

H. G. Sander  
I. Phys. Institut, TH Aachen

T. F. Walsh  
Deutsches Elektronen-Synchrotron DESY, Hamburg

P. M. Zerwas  
Inst. f. Theor. Physik, TH Aachen +  
and DESY, Hamburg

+ permanent address

I. Introduction

Three jets in the hadronic final states of  $e^+e^-$  annihilation have recently been observed at PETRA /1/. These events are naturally explained in quantum chromodynamics (QCD) as due to gluon bremsstrahlung off a quark-antiquark pair,

$$e^+ e^- \rightarrow q\bar{q}G \rightarrow 3 \text{ hadron jets.} \quad (1)$$

In fact, reaction (1) was suggested a long time ago as a potential test of QCD at short distances /2/.

Distributions of global quantities like sphericity, thrust, jet broadening etc. have been worked out for perturbative gluon bremsstrahlung in great detail (see /3/ and references quoted therein). Where comparisons exist, the QCD predictions of Ref. /3/ are in remarkably good agreement with the data. It appears that gluons exist and that QCD is substantiated. But it is important to show that the "gluon" in (1) has spin 1. Our aim in this paper is thus to discuss the angular correlations of low thrust ( $T \lesssim 0.9$ ) three-jet events, which are a fraction  $O(\alpha_s/\pi) \sim 10\%$  of all hadronic annihilation events. We expand on earlier work /4/ in

three points. (i) We investigate polarization effects for transversely as well as longitudinally polarized lepton beams. (ii) We confront the angular asymmetries predicted by QCD with a scalar gluon "theory". This is done to show how much of the asymmetry is due to the spin 1 nature of the gluon in QCD, and how much might be merely a consequence of the

kinematics of gluon radiation. /+/ (iii) We estimate numerically how finite transverse momenta in the jet fragmentation affect the angular asymmetries (the admixture of 2 jet events is included).

The angular asymmetries we discuss are typically of the order of 10 %, requiring a rather large sample of 3 jet events to allow for statistically significant results. /++/ Nevertheless, asymmetries averaged over thrust values  $T \sim 0.7$  to  $0.9$  should be measurable in the near future. They will provide an indispensable link between three-jet events in the  $e^+e^-$  continuum and quantum chromodynamics.

We organize the material as follows. First we present the cross section ( $e^+e^- \rightarrow q\bar{q}G$ ) for transversely and longitudinally polarized lepton beams. Several asymmetries can be defined for 3-quantum final states. (Forward-backward asymmetry of the thrust axis; left-right asymmetry of the second fastest jet with respect to the plane formed by the thrust axis and the lepton beam axis; etc.) These asymmetries can be expressed in terms of three parameters which are completely determined in QCD perturbation theory. Next we determine the asymmetry parameters for pions which are fragments of gluon and quark jets. We confront the QCD results with those obtained in a scalar gluon theory. Finally we study how much the asymmetries are

/+/ Just remember that the polar angle distribution of the normal to a continuum  $e^+e^-$  event does not test QCD. It is the same for scalar and vector gluons, and even accidentally "flat"  $q\bar{q}$  jet events have this same distribution of the normal. (namely  $3 - \cos^2\theta_N$ ) /5/ /++/ By contrast, the thrust axis distribution in onium decays shows an easily visible difference between QCD and a model with scalar gluons /6/. It is thus a clean QCD test. (Curiously, for onium decays the distribution of the normal to the event plane does differ for vector and scalar gluons /7/.)

affected by nonperturbative effects (finite transverse momenta in the jet fragmentation, etc.).

II. Angular Asymmetries in 3-Jet Events

A three-jet event in  $e^+e^-$  annihilation can be characterized by two energies and three angles (see Fig. 1a,b): (i) The energies of the quark and anti-quark jet,  $x_q$  and  $x_{\bar{q}}$ , measured in units of the beam energy. The gluon jet energy is then  $x_g = 2 - x_q - x_{\bar{q}}$ . (ii) The angles are: first, the polar angle  $\theta$  between the electron direction and the thrust direction (defined by the momentum of the most energetic jet). Second, the angle  $\varphi$  between the projections of the electron spin vector  $s(e^-)$  and the thrust direction in the plane perpendicular to the lepton beams. And finally, the angle  $\chi$  between the jet plane and a plane formed by the thrust axis and the lepton beam axis, the direction being defined by the 2nd most energetic jet and the  $e^+$  momentum.

The helicity analysis of one-photon annihilation shows that the differential cross section for  $e^+e^- \rightarrow q\bar{q}g$  can be written as follows /6/

$$\begin{aligned}
 (2\pi)^2 \frac{d\sigma}{d\cos\theta dx d\varphi} = & \\
 = & \frac{3}{8} \left[ (1 - P_{11}^2)(1 + \cos^2\theta) - P_1^2 \sin^2\theta \cos 2\varphi \right] \sigma_U + \\
 & + \frac{3}{4} \left[ (1 - P_{11}^2) + P_1^2 \cos 2\varphi \right] \sin^2\theta \sigma_L \\
 & + \frac{3}{4} \left[ \left\{ (1 - P_{11}^2) \sin^2\theta - P_1^2 (1 + \cos^2\theta) \cos 2\varphi \right\} \cos 2\chi + \right. \\
 & \quad \left. + 2P_1^2 \cos\theta \sin 2\chi \sin 2\varphi \right] \sigma_T \\
 & - \frac{3}{\sqrt{2}} \left[ (1 - P_{11}^2 + P_1^2 \cos 2\varphi) \cos\theta \cos\chi - P_1^2 \sin\chi \sin 2\varphi \right] \sin\theta \sigma_I
 \end{aligned}
 \tag{2}$$

$P_{11}, P_{\perp}$  denote the parallel/perpendicular polarization of the electron with respect to its momentum (we take  $\vec{s}(e^+) = -\vec{s}(e^-)$ ). The  $\sigma$ 's are differential cross sections in the energies,  $\sigma \equiv d\sigma/dx_q dx_{\bar{q}}$ ; they correspond to the following photon spins:

- U = unpolarized transverse
- L = longitudinally polarized
- I = transverse/longitudinal interference term
- T = +/- interference term

The cross section (2) can be experimentally evaluated in several steps of increasing complexity.

1) Angular distribution of the thrust axis

Measuring only the polar angle of the thrust axis (and not the direction of the 2nd fastest jet) one arrives at

$$\frac{d\sigma}{d\cos\theta} = \frac{3}{8} \left[ 1 + \alpha \cos^2\theta \right] (1 - P_{11}^2) (\sigma_U + 2\sigma_L)
 \tag{3}$$

The parameter  $\alpha$ ,

$$\alpha = \frac{\sigma_U - 2\sigma_L}{\sigma_U + 2\sigma_L}
 \tag{4}$$

describes the strength of the longitudinal cross section  $\sigma_L$  relative to the transverse cross section  $\sigma_U$ . Pointlike quark-antiquark pair production gives  $\alpha = 1$ . Measuring  $\alpha$  through the polar angle distribution

of the thrust axis is independent of the polarization of the lepton beams; longitudinal beam polarization merely affects the overall magnitude of the cross section.

If the lepton beams have a transverse polarization component one can use the  $\psi$  asymmetry of the thrust axis to determine  $\alpha$ . Defining  $A_\psi$  as the number of events with  $|\psi|$  or  $|\pi - \psi| \leq \pi/4$  minus the number of events with  $|\pi/2 - \psi|$  or  $|3\pi/2 - \psi| \leq \pi/4$  (normalized to the sum) one readily obtains

$$A_\psi = -\frac{2}{\pi} \frac{P_\perp^2}{1 - P_\parallel^2} \frac{\sin^2 \theta}{1 + \alpha \cos^2 \theta} \alpha \quad (5)$$

If the thrust axis is perpendicular to the lepton beams,  $\theta = \pi/2$ ,  $A_\psi$  is proportional to  $\alpha$ .

2) Angular asymmetries of the 2nd fastest jet

The longitudinal and transverse interference term  $\sigma_T$  and  $\sigma_I$  in the 3-jet cross section (2) can be isolated by measuring the angular distribution of the 2nd fastest jet  $\chi$ . Defining the ratio

$$\beta = \frac{2\sigma_T}{\sigma_U + 2\sigma_L} \quad (6)$$

we count the number of events with  $|\chi|$  or  $|\pi - \chi| \leq \pi/4$  minus the number of events with  $|\pi/2 - \chi|$  or  $|3\pi/2 - \chi| \leq \pi/4$  (normalized to the

total event number). This is

$$A_B = +\frac{2}{\pi} \frac{\sin^2 \theta}{1 + \alpha \cos^2 \theta} \beta \quad (7)$$

(B = "Beamness"). It is independent of the lepton beam polarization and is a maximum for the thrust axis perpendicular to the  $e^+$  momentum.

Likewise, a forward-backward asymmetry  $A_{FB}$  can be measured,  $|\chi|$  or  $|\pi - \chi| \leq \pi/2$ ,

$$A_{FB} = +\frac{2}{\pi} \frac{\sin 2\theta}{1 + \alpha \cos^2 \theta} \gamma \quad (8)$$

with  $\gamma$  describing the transverse/longitudinal interference part of the cross section,

$$\gamma = \frac{-2\sqrt{2}\sigma_I}{\sigma_U + 2\sigma_L} \quad (9)$$

This forward-backward asymmetry is a maximum for polar angles of the thrust axis  $\theta = 45^\circ$  and  $135^\circ$  (hampering the measurement of  $\sigma_I$  through  $A_{FB}$  in detectors of limited acceptance in  $\theta$ ).

3) Combining  $\chi$  and  $\psi$  asymmetries

A transverse polarization component of the lepton beams allows the measurement

of many more asymmetries. (Of course, there are still only four  $\sigma^i$ .) Denoting the difference of the number of events with  $\cos \chi \cos 2\varphi > 0$  vs.  $\cos \chi \cos 2\varphi < 0$  by  $N_r [\cos \chi \cos 2\varphi \gtrless 0]$  etc., normalized to the total number of events, we have listed all possibilities in Table 1.

Special attention ought to be paid to the last row in this table. It describes a valuable alternative for measuring  $\sigma_T$  by using beam polarization (especially if the detectors have a limited acceptance in the polar angle  $\theta$ ).

Without employing beam polarization effects, one can of course still determine the asymmetry parameter  $\alpha, \beta$  and  $\chi$  using the three different angular distributions of the thrust axis and the second fastest jet. Beam polarization provides a wealth of independent information which greatly helps complement and cross check the former measurements.

## II. QCD Predictions of $\alpha, \beta$ and $\chi$ for Jets

First order perturbative quantum chromodynamics predicts  $\alpha, \beta$  and  $\chi$  in  $e^+e^- \rightarrow q\bar{q}G$  without any free parameter. The only free parameter of perturbative QCD, the scale  $\Lambda$  of the running quark-gluon coupling constant, drops out when taking ratios. Angular correlations are, therefore, an exceedingly clean testing ground for quantum chromodynamics. Just to develop an idea of how much of the behaviour of  $\alpha, \beta, \chi$  is due to 3 jet kinematics we confront the QCD case with spin 1 gluons to a fake "theory" with massless spin 0 quanta (scalar and pseudoscalar gluons give identical results when masses are neglected).

The QCD results for  $d\sigma_i/dx_q dx_g$  ( $i = U, L, I, T$ ) have been calculated in

Ref. /4/ and those for scalar gluons in Ref. /3/. We write for a quark species of charge  $e_q$

$$\frac{d\sigma_i}{dx_q dx_g} = \frac{4\pi\alpha^2 e_q^2}{s} \frac{2\alpha_s}{\pi} \frac{S_i(x_q, x_g, x_{\bar{q}})}{(1-x_q)(1-x_g)} \quad (10)$$

with  $\sqrt{s}$  being the total CM energy and  $\alpha_s = g_s^2/4\pi$  denoting the quark-gluon coupling constant. The coefficients  $S_i$  are collected in Table 2 for vectorial and scalar gluons. In the first column the thrust axis (taken as quantization axis for the photon spin) is given by the momentum of the quark and in the second column by the momentum of the gluon. <sup>/+/</sup> Charge conjugation invariance tells us that the coefficients for  $T = \bar{q}$  are obtained from the first column by interchanging  $x_q$  and  $x_g$ . Recall  $\cos \theta_{ij} = 1 + 2(1-x_i-x_j)/x_i x_j$  and  $x = +2 \left[ (1-x_q)(1-x_g)(1-x_G) \right]^{1/2} / T$ . (note that here  $T = \text{thrust}$ )

Since  $\sigma_L = 2\sigma_T$  holds in the massless quark and gluon limit (the equality fails if finite quark masses are introduced /9/), the following relation obtains between  $\alpha$  and  $\beta$ ,

$$\alpha = 1 - 4\beta \quad (11)$$

leaving us with only two independent asymmetry parameters.

Inspection of Table 2 shows that the angular distributions of 3-jet events in quantum chromodynamics are clearly distinct from other possibilities, if the quark and gluon jets could be identified. Since this is difficult in the

<sup>/+/</sup> The angle  $\chi$  is defined by the antiquark in the first case and by the quark in the second case.

present energy range, we turn to the less ambitious question of angular distributions of the thrust axis and the axis of the second fastest jet for a given thrust value of the event.

Cross sections and interference terms in Eq. (2) for a thrust value

$T = \max(x_q^+, x_q^-, x_c)$  read as follows:

(i) Quantum chromodynamics /4/:

$$\frac{d\sigma^L}{dT} = \sigma_1 \left[ \frac{2(3T^2 - 3T + 2)}{T(1-T)} \ln \frac{2T-1}{1-T} - \frac{3(3T-2)(2-T)}{1-T} - \frac{2(8T-3T^2-4)}{T^2} \right] \quad (12)$$

$$\frac{d\sigma^L}{dT} = 2 \frac{d\sigma^T}{dT} = \sigma_1 \frac{2(8T-3T^2-4)}{T^2}$$

$$\frac{d\sigma^I}{dT} = -\sigma_1 \sqrt{2} (2-2T+T^2) \left[ \frac{1}{T\sqrt{1-T}} - \frac{2}{T^2} \sqrt{2T-1} \right]$$

(ii) Scalar gluons:

$$\frac{d\sigma^U}{dT} = \sigma_1 \frac{3}{8} \left[ \frac{(3T-2)(4-3T)}{1-T} + 2 \ln \frac{2T-1}{1-T} - \frac{2(3T-2)}{T} \right]$$

$$\frac{d\sigma^L}{dT} = 2 \frac{d\sigma^T}{dT} = \sigma_1 \frac{3}{4} \frac{3T-2}{T}$$

$$\frac{d\sigma^I}{dT} = -\sigma_1 \frac{3}{4\sqrt{2}} \left[ \sqrt{1-T} - \frac{2(1-T)}{T} \sqrt{2T-1} \right]$$

The common factor  $\sigma_1$  is defined as

$$\sigma_1 = \frac{4\pi\alpha^2 e_q^2}{s} \frac{2\alpha_s}{3\pi}$$

for a quark species of charge  $e_q$ . These functions are shown in Fig. 2.

To fix the running coupling constant of QCD we assumed 4 quark flavors,

$\sqrt{s} = 30$  GeV and  $\Lambda = \frac{1}{2}$  GeV. The scalar gluon-quark coupling constant was fixed by requiring  $(d\sigma^U/dT)_{\text{SCALAR}} = (d\sigma^U/dT)_{\text{QCD}}$  at  $T = 0.8$ , qualitatively suggested by the data of Refs. /1/.

A few remarks concerning the comparison between QCD and the scalar theory are appropriate. (i) The longitudinal part of the cross section is more important in scalar than vector theories. (ii) The interference term is divergent in QCD for  $T \rightarrow 1$ , whilst vanishing at this point in scalar gluon theories.

We are now in a position to discuss the (parameter-free) asymmetries  $\alpha$ ,  $\beta$  and  $\gamma$  for a given thrust value  $T$  of the events (Figs. 3a,b and c).

(i)  $\alpha(T)$  in Fig. 3a starts at 1 for  $T = 1$  and falls monotonically to  $\frac{1}{3}$  at  $T = \frac{2}{3}$ . The fall-off in the scalar gluon case is faster for large  $T$  and in the most interesting region of  $T$  between 0.8 and 0.9 the values of  $\alpha$  differ by approximately a factor of 2.

(ii) According to Eq. (11),  $\beta(T)$  in Fig. 3b must rise from 0 to  $\frac{1}{3}$  by going from  $T = 1$  down to  $T = \frac{2}{3}$ . The average magnitude of  $\beta$  in the thrust range below 0.8 is larger than 10% in QCD.

(iii) Fortunately enough,  $\gamma(T)$  in Fig. 3c has got a broad maximum of the order of 10% in QCD, whilst being much smaller for scalar gluons.



The asymmetry parameters  $\alpha_s$ ,  $\beta$  and  $\gamma$  for jet distributions shown in Fig. 3 are the result of perturbative QCD and scalar gluon calculations on the quantum level. Finite transverse momentum effects and mass effects during the fragmentation process of the quark and gluon quanta into hadrons are not yet taken account of. It is qualitatively clear, however, in which way these effects change the behavior of the asymmetries. The nonperturbative effects will shift the curves slightly towards smaller thrust values (the measured thrust value of an event corresponds to a larger thrust value on the quark/gluon level). We will study this shift quantitatively in the fourth section.

### III. Pion Asymmetries

In the preceding section we have discussed asymmetry effects in angular distributions of quark and gluon jets - generally considered to be the most direct way of testing perturbative QCD in the "femto-universe" /10/. In the following, we extend the QCD predictions to single hadrons by adopting the fragmentation picture for quark and gluon jets. We will study  $\pi^+ = \frac{1}{2}(\pi^+ + \pi^-)$  distributions only and assume a universal fragmentation function  $\xi D(\xi) = (1-\xi)^2$  for  $\pi^+$ 's carrying away a fraction  $\xi$  of the quark or gluon momentum.

1) The most general form of the polar angle distribution of  $\pi^+$ 's in

$$e^+e^- \rightarrow \pi + \text{anything}, \quad (14)$$

with fixed thrust value T, is

$$\frac{d\sigma}{d\cos\theta} \propto 1 + \alpha_T(\mathbf{z}) \cos^2\theta \quad (15)$$

The same  $\alpha_T(\mathbf{z})$  appears in the  $\psi$  asymmetry of the  $\pi^+$ 's - completely analogous to Eq. (5):

$$A_\psi(\pi) = -\frac{2}{\pi} \frac{p_T^2}{1-p_T^2} \frac{\sin^2\theta}{1+\alpha_T(\mathbf{z})\cos^2\theta} \alpha_T(\mathbf{z}) \quad (16)$$

Gluon theories complemented by the fragmentation hypothesis predict  $\alpha_T(\mathbf{z})$ . Since we neglect nonperturbative transverse momentum effects in the jet fragmentation we have to restrict the  $\mathbf{z}$  range to  $\mathbf{z} \geq O(1)$ .  $\alpha_T(\mathbf{z})$  is found by evaluating the ratio

$$\alpha_T(\mathbf{z}) = \frac{\sigma_U(\pi) - 2\sigma_L(\pi)}{\sigma_U(\pi) + 2\sigma_L(\pi)} \quad (17)$$

for the unpolarized transverse and longitudinal single  $\pi$  cross sections,  $\sigma_U(\pi)$  and  $\sigma_L(\pi)$ , respectively. They are given by summing over all jets as sources for  $\pi^+$ 's when the quark or the antiquark or the gluon defines the thrust axis. Introducing from Table 2

$$\rho_i(j; x_q, x_g, x_c) = \frac{S_i(x_q, x_g, x_c)}{(1-x_q)(1-x_g)} \quad (18)$$

for  $i = U, L, T, I$  and  $j = q, \bar{q}, G$  denoting the quantization axis (called T(1) in Table 2), we readily obtain

$$\begin{aligned} \sigma_i(\pi) \propto & \int_a^T dx \left\{ 2\rho_i(q; T, x, 2-T-x) + \rho_i(G; x, 2-T-x, T) \right\} \frac{D(z/T)}{T} \\ & + 2 \int_a^T dx \left\{ \rho_i(q; x, T, 2-T-x) + \rho_i(q; x, 2-T-x, T) \right\} \\ & + \rho_i(G; T, 2-T-x, x) \left\} \frac{D(z/T)}{x} \end{aligned} \quad (19)$$

with  $a = \max [2(1-T), z]$  and, of course,  $z$  (the fraction of beam energy carried away by  $\pi$ )  $\leq T$ .

$\alpha_T(z)$  is shown for three thrust values in Fig. 4a and b, for QCD and for scalar gluons, respectively. For large  $z$  in each thrust line, the distributions clearly reflect the thrust axis distribution. Decreasing  $z$ , they become more and more isotropic. This tendency is of course reinforced if finite transverse momenta are introduced in the jet fragmentation.

2) To define the asymmetries  $\beta_T(z)$  and  $\gamma_T(z)$  we divide each annihilation event into a thin-jet and a fat-jet part  $/3/$ . Out of the latter two separate jets emerge for sufficiently large energy and small thrust  $/1/$ . We consider the  $X$  distribution of the pions in the fat jet around the thrust axis (the rôle of the second fastest jet in Fig. 1a is taken over by the  $\pi$ 's),

$$e^+ e^- \rightarrow \text{thin jet} + \text{fat jet} \rightarrow \pi + \text{anything} \quad (20)$$

Azimuthal angular asymmetries can now be defined for  $\pi$ 's analogously to Eqs. (7,8) and those in Table 2. We have

$$\beta_T(z) = \frac{2 \sigma'_T(\pi)}{\sigma'_U(\pi) + 2 \sigma'_L(\pi)} \quad (21)$$

and

$$\gamma_T(z) = \frac{-2\sqrt{z} \sigma'_z(\pi)}{\sigma'_U(\pi) + 2 \sigma'_L(\pi)} \quad (22)$$

if the thrust is given by the quark's momentum, the antiquark and the gluon define the fat jet, serving as sources for the analyzed  $\pi$ 's, etc. The cross sections and interference terms  $\sigma'_i(\pi)$ , therefore, read

$$\begin{aligned} \sigma'_i(\pi) \propto & \int_a^T dx \left\{ 2\rho_i(q; T, x, 2-T-x) + \rho_i(G; x, 2-T-x, T) \right\} \frac{D(z/T)}{x} \\ & + \epsilon_i \int_{2(1-T)}^T dx \left\{ 2\rho_i(q; T, x, 2-T-x) + \rho_i(G; x, 2-T-x, T) \right\} \frac{D(z/(2-T-x))}{2-T-x} \end{aligned} \quad (23)$$

for  $i = U, L, T$ , with  $\epsilon_{U, L, T} = +1$  and  $\epsilon_T = -1$ ;  $a = \max [2(1-T), z]$  and  $b = \min [T, 2-T-z]$ .

$\beta_T(z)$ , in Figs. 5a and b, is only a bit dependent on  $z$  whereas the  $T$  dependence follows closely  $\beta(T)$  in Fig. 3b. Nonperturbative transverse momentum effects bend the curves to zero, of course, at small  $z$ .

$\gamma_T(z)$ , on the other hand, appears strongly  $z$  dependent (see Figs. 6a and b), reflecting the  $T$  dependence of  $\gamma(T)$  only for  $z \sim T$ . At  $z = 0$ ,  $\gamma_T(0) = 0$ . This is a consequence of contributions of opposite signs to  $\langle \cos X \rangle$ ,

coming from the  $\bar{q}$  and  $C$  jet if  $q$  defines the thrust axis, etc. Assuming universal fragmentation function for all jets, as we did, leads to exact cancellation at  $z = 0$ . It is clear that  $\gamma_T(z)$  is vulnerable to changes of quark and gluon-fragmentation functions at small  $z$ .

In the following section we will describe how those results become (slightly) modified if finite mass and transverse momentum effects are incorporated in the jet fragmentation.

#### IV. Estimating Nonperturbative Effects

Finite mass effects and nonperturbative transverse momentum effects are most easily described by imposing the Field-Reynan fragmentation model /11/ on the quark pair and the quark-gluon production cross section. We will employ again the simple Monte Carlo model developed in Ref. /3/. The model introduces  $u$ ,  $d$  and  $s$  quarks only, and we assume a perfect experimental reconstruction of the theoretical thrust axis (and the axis of the 2nd fastest jet if necessary).

The parameter  $\alpha(T)$  is affected by nonperturbative jet formation in the following way. Quark-antiquark jet production contributes significantly to the thrust range down to  $T \approx 0.85$  for CM energy  $\approx 30$  GeV. These events carry the theoretical  $\alpha$  value 1. In addition, the measured thrust value is always smaller than the perturbative thrust value on the quark-gluon level in 3-jet events. Both mechanisms raise the curves  $\alpha(T)$  slightly over the perturbative values shown in Fig. 3a. We display the results of the model in Table 3. Two points are worth stressing. (i) For all  $T \lesssim 0.8$ ,  $\alpha$  is much smaller in QCD than the parton value 1. And (ii), over the whole  $T$  range  $\lesssim 0.9$  scalar gluon

theories predict an appreciably smaller value for  $\alpha$  than does QCD.

Quark-antiquark pair production decreases the  $\chi$  asymmetries  $\beta$  and  $\gamma$  by adding to the denominators of the ratios (6) and (9), but not contributing to their numerators. For the 3-jet final states we have again an effective lowering of the  $T$  values by nonperturbative mechanisms. As a result we expect a shift of the perturbative curves  $\beta(T)$  and  $\gamma(T)$  in Fig. 3b and c to the left. This is born out by the numbers displayed in Table 3.

We close this section by presenting a Monte Carlo study of the inclusive single  $\pi$  asymmetries  $\alpha_T(z)$ ,  $\beta_T(z)$  and  $\gamma_T(z)$  in Table 4a, b and c, respectively. The same tendency observed when comparing Fig. 4 with Table 3 is also evident here. In addition, in the lowest  $r$  bin the numbers are substantially lower than the pure perturbative calculation, as anticipated from the chaotic character of slow particle distributions. /+/

+/+ Comparing  $\gamma_T(z)$  in Fig. 6a with the numerical values in Table 4c again shows how sensitive this asymmetry is to the details of the fragmentation mechanism.

V. Summary

We think it important to prove that the three jet events seen at PETRA are due to the radiation by quarks of a flavorless vector quantum. Establishing the vector nature of the gluon would put this particle on the same footing as the spin 1/2 quarks. The analysis presented here shows in some detail how this can be done. Perhaps one of the best ways is simply to measure the angular distribution of the thrust axis, used originally at T<sub>2</sub>1 to show that quarks have spin 1/2. At lower thrust, the angular distribution of three jet events is a test that the radiated gluon has spin = 1. We have also presented other asymmetries (there are three in all, including that just mentioned).

In judging how sharply angular distributions test QCD, it is useful to have an ad hoc alternative. So we compared QCD to a fake "theory" with massless scalar gluons. A discrimination is possible, given sufficient data at low thrust. It is thus clear that angular distributions form a clear test of QCD, sensitive to the vectorial nature of gluons.

Acknowledgement

We gratefully acknowledge a discussion with E. Laermann, K.K. and P.H.Z. thank Hans Joes for the warm hospitality extended to them by DESY.

References

/1/ R. Brandelik et al. (TASSO Collaboration), Phys. Lett. 86B (1979) 243;  
 D.P. Barber et al. (MARK-J Collaboration), Phys. Rev. Lett. 43 (1979) 830;  
 C. Berger et al. (PLUTO Collaboration), Phys. Lett. 86B (1979) 418.  
 S. Orto, DESY Preprint 79/77  
 /2/ J. Ellis, M.K. Gaillard and G. Ross, Nucl. Phys. B111 (1976) 25  
 T. DeGrand, Y.J. Ng and S.-H. Tye, Phys. Rev. D16 (1977) 3251.  
 /3/ P. Hoyer et al., DESY report 79/21.  
 /4/ G. Kramer, C. Schierholz and J. Willrodt, Phys. Lett. 79B (1978) 249  
 and E 80B (1979) 433.  
 /5/ G. Fox and S. Wolfram, Gallimauftric comment.  
 /6/ K. Koller and H. Krasemann, DESY preprint  
 /7/ K. Koller and T.F. Walsh, Nucl. Phys. B140 (1978) 449.  
 /8/ N.M. Avram and D.H. Schiller, Nucl. Phys. B70 (1974) 272.  
 /9/ E. Laermann and P.H. Zerwas, Aachen preprint (Sept. 1979).  
 /10/ J.D. Bjorken, SLAC Summer Institute 1979.  
 /11/ R. Field and R.P. Feynman, Nucl. Phys. B136 (1978) 1.

Definition	Asymmetry
Nr. $[\cos 2\chi \cos 2\psi \geq 0]$	$A'_B = -\xi \frac{1 + \cos 2\theta}{1 + \alpha \cos 2\theta} \beta$
Nr. $[\sin 2\chi \sin 2\psi \geq 0]$	$A''_B = +\xi \frac{2 \cos \theta}{1 + \alpha \cos 2\theta} \beta$
Nr. $[\cos \chi \cos 2\psi \geq 0]$	$A'_{FB} = +\xi \frac{\sin 2\theta}{1 + \alpha \cos 2\theta} \gamma$
Nr. $[\sin \chi \sin 2\psi \geq 0]$	$A'_{LR} = -\xi \frac{2 \sin \theta}{1 + \alpha \cos 2\theta} \gamma$

Table 1: Asymmetries resulting from transverse beam polarization. The first column defines the events which are counted positive or negative depending on the value  $\chi$  of the second fastest jet in Fig. 1a and the angle  $\psi$  of the thrust axis with respect to the transverse component of the  $e^-$  spin vector in Fig. 1b.  $\xi$  abbreviates the polarization factor  $(2M^2)^2 P_1^2 / (1 - P_1^2)$

	T = q	T = G
QCD		
U	$x_q^2 + x_{\bar{q}}^2 - \frac{1}{2} x_1^2$	$x_q^2 + x_{\bar{q}}^2 - x_1^2$
L = 2T	$\frac{1}{2} x_1^2$	$x_1^2$
I	$\frac{1}{2\sqrt{2}} x_1 x_{\bar{q}} \cos \theta_{q\bar{q}}$	$\frac{1}{2\sqrt{2}} x_1 [x_q \cos \theta_{qG} - (q \rightarrow \bar{q})]$
Scalar gluons		
U	$\frac{3}{8} [x_G^2 - \frac{1}{2} x_1^2]$	$\frac{3}{8} x_G^2$
L = 2T	$\frac{3}{16} x_1^2$	0
I	$-\frac{3}{16\sqrt{2}} x_1 x_G \cos \theta_{qG}$	0

Table 2: Coefficients of the helicity cross sections for QCD and scalar gluons. T = q is obtained by interchanging q and  $\bar{q}$  in the first column.

	0.7	0.8	0.9	1.0
$\alpha(T)$	0.45	0.67	0.94	0.99
QCD	0.38	0.48	0.79	0.99
SCALAR	0.12	0.06	0.02	0.00
$\beta(T)$	0.16	0.14	0.06	0.00
QCD	0.08	0.11	0.06	0.00
SCALAR	0.06	0.04	0.02	0.00
$\gamma(T)$				

Table 3:  $\alpha$ ,  $\beta$  and  $\gamma$  in four thrust bins. The Field-Feynman jet fragmentation is applied to  $q\bar{q}$  and  $q\bar{q}G$  quantum final states.

(a)  $\alpha_T(z)$

	0.8	0.9	1.0
$0.05 \leq z < 0.1$	0.28	0.57	0.80
QCD			
$0.1 \leq z < 0.2$	0.24	0.52	0.81
SCALAR			
QCD	0.42	0.79	0.97
SCALAR	0.29	0.70	0.96
$0.2 \leq z < 1$	0.51	0.88	1.00
QCD			
SCALAR	0.29	0.74	1.00

(b)  $\beta_T(z)$

	0.8	0.9	1.0
$0.05 \leq z < 0.1$	0.04	0.01	0.00
QCD			
$0.1 \leq z < 0.2$	0.12	0.03	0.00
SCALAR			
QCD	0.05	0.02	-0.01
SCALAR	0.11	0.04	0.00
$0.2 \leq z < 1$	0.13	0	0.01
QCD			
SCALAR	0.15	0.06	0.01

(c)  $\gamma_T(z)$

	0.8	0.9	1.0
$0.05 \leq z < 0.1$	0.00	0.00	0
QCD			
$0.1 \leq z < 0.2$	0.04	0.01	0
SCALAR			
QCD	0.04	0	0
SCALAR	0.02	0.01	0
$0.2 \leq z < 1$	0.04	0.04	0.01
QCD			
SCALAR	-0.02	-0.02	0

Tables 4:  $\alpha_T(z)$ ,  $\beta_T(z)$  and  $\gamma_T(z)$  when taking account of  $q\bar{q}$  pair production and nonperturbative jet fragmentation.

Figure Captions

Fig. 1a: The co-ordinate system for a three-jet event.

Fig. 1b: Components of the spin vector and the momentum vector of one of the jets in the plane perpendicular to the beams.

Fig. 2: The cross sections  $d\sigma_i/dT$ ,  $i = U, L, I$  for vector and scalar gluons (solid and dashed lines). Note that  $d\sigma_U = 2d\sigma_T$  for both vector and scalar gluons.

Fig. 3a: Plot of  $\alpha(T)$ . For unpolarized beams, the thrust axis distribution is  $\propto 1 + \alpha(T) \cos^2\theta$ .  $\alpha(T)$  can also be measured through  $\psi$  distributions.

Fig. 3b: Plot of the  $\beta(T)$ . This describes the tendency of the  $q\bar{q}G$  plane to lie parallel to the beam axis.

Fig. 3c: Plot of  $\gamma(T)$ . This describes the tendency of the second most energetic jet to lie near the beam direction.

Fig. 4a: Plot of  $\alpha_T(z)$  for fixed thrust  $T = .7, .8, .9$ . is the scaled inclusive hadron momentum.

Fig. 4b: The same for scalar gluons

Fig. 5a: Plot of  $\beta_T(z)$ , for  $T = .7, .8, .9$  as in Fig. 4a.

Fig. 5b: The same for scalar gluons

Fig. 6a: Plot of  $\gamma_T(z)$ , for  $T = .7, .8, .9$  as in Fig. 4a.

Fig. 6b: The same for scalar gluons

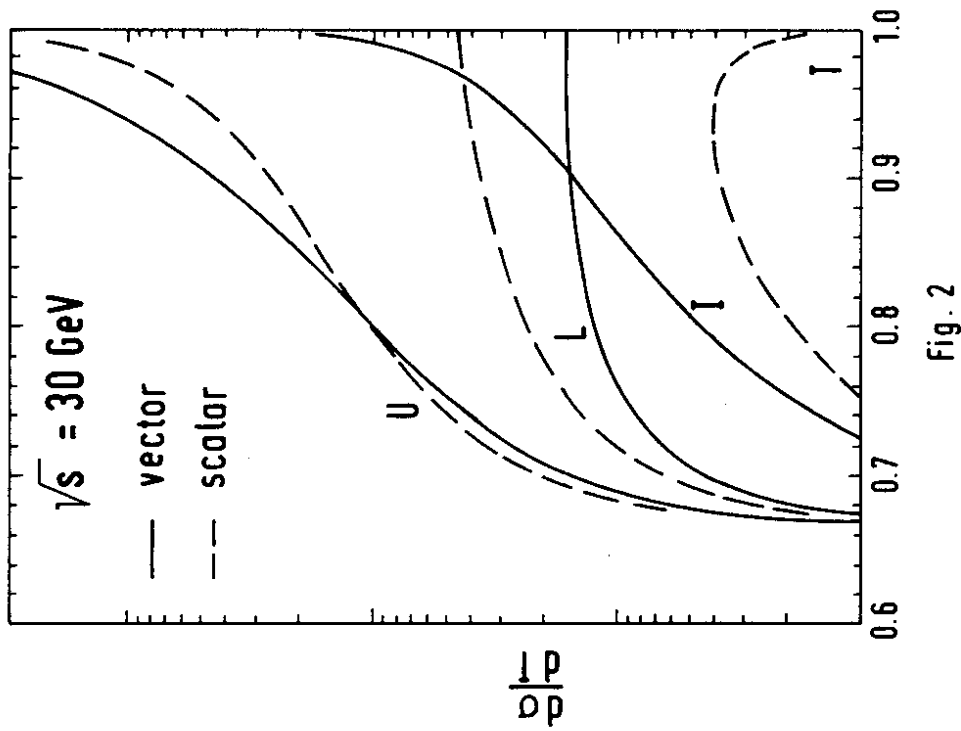


Fig. 1a

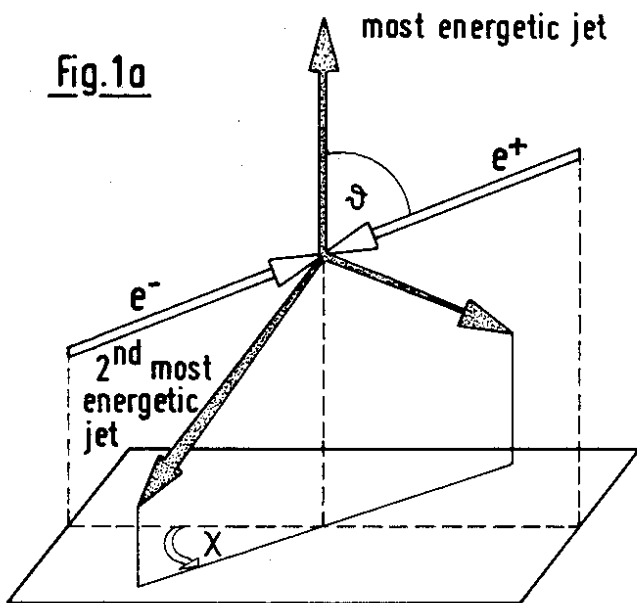
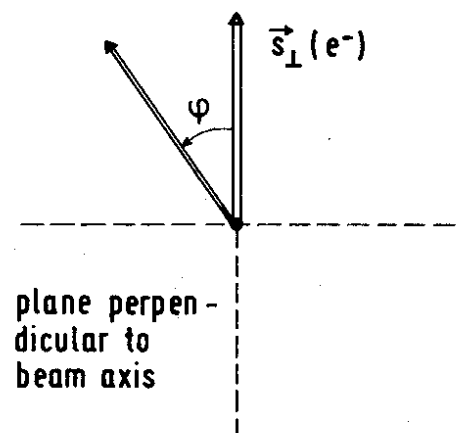


Fig. 1b





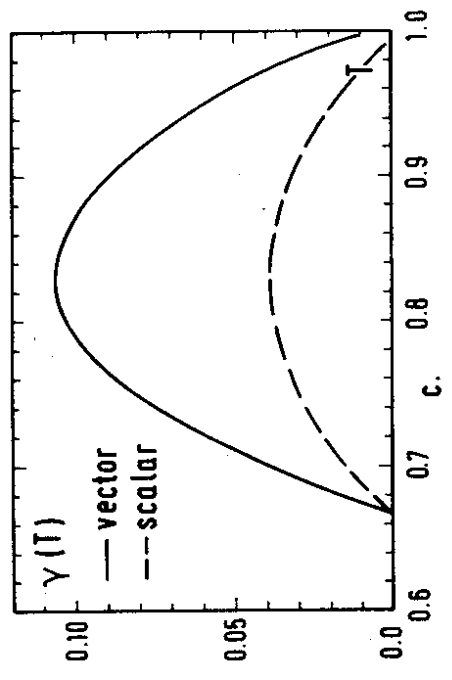
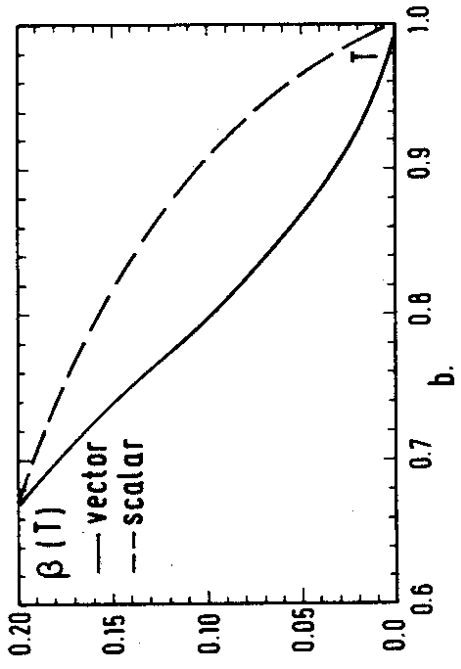
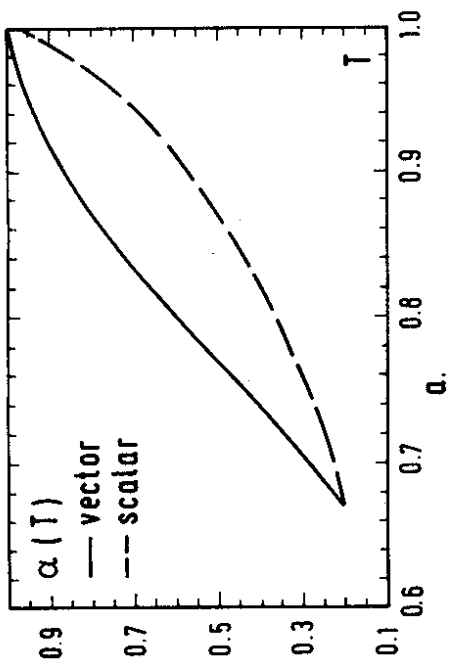
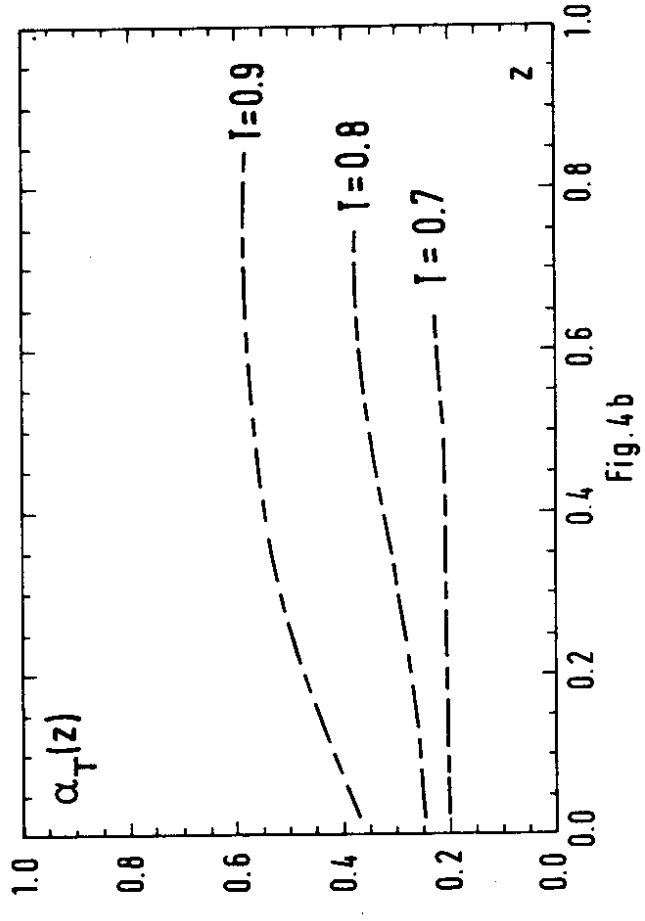
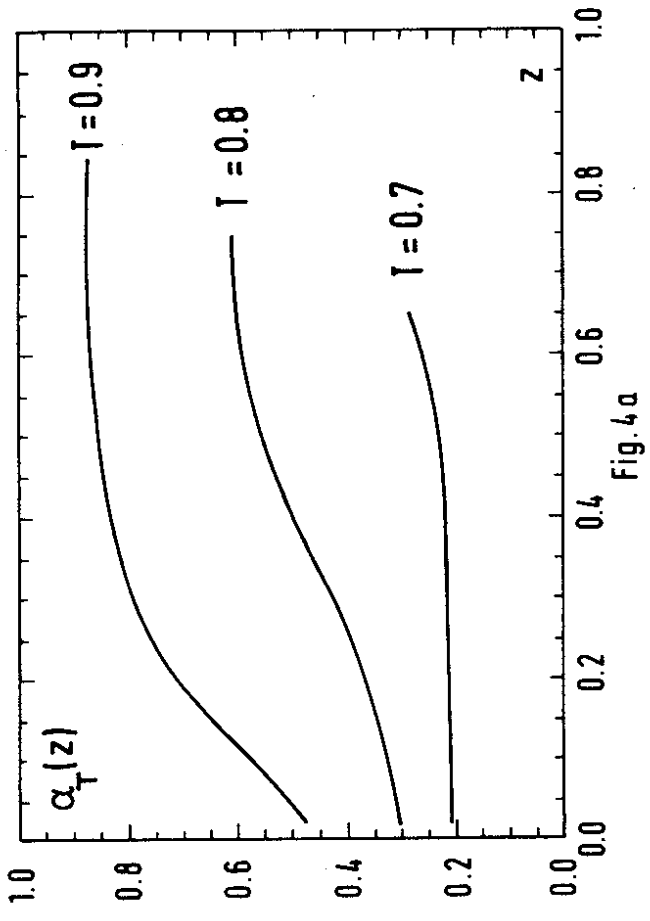


Fig. 3



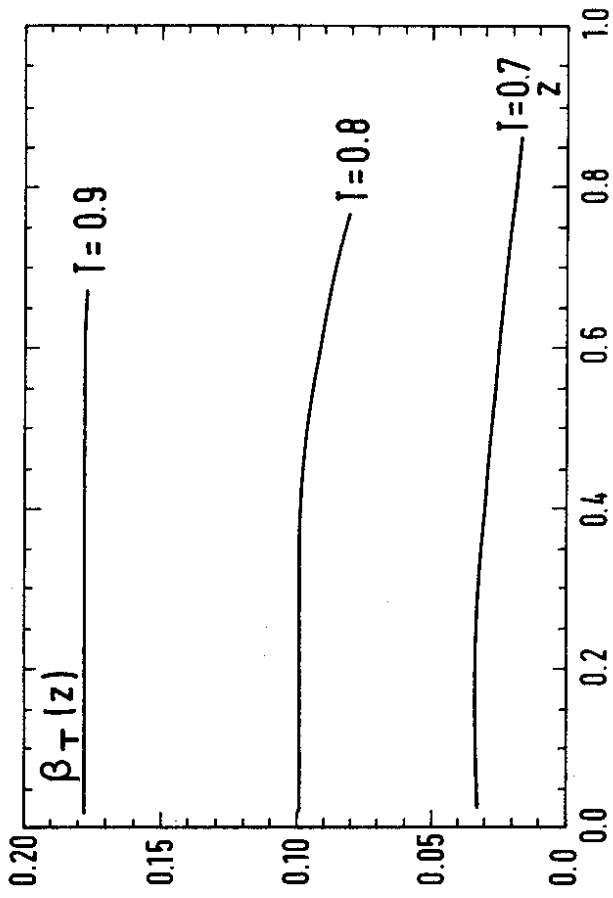


Fig. 5a

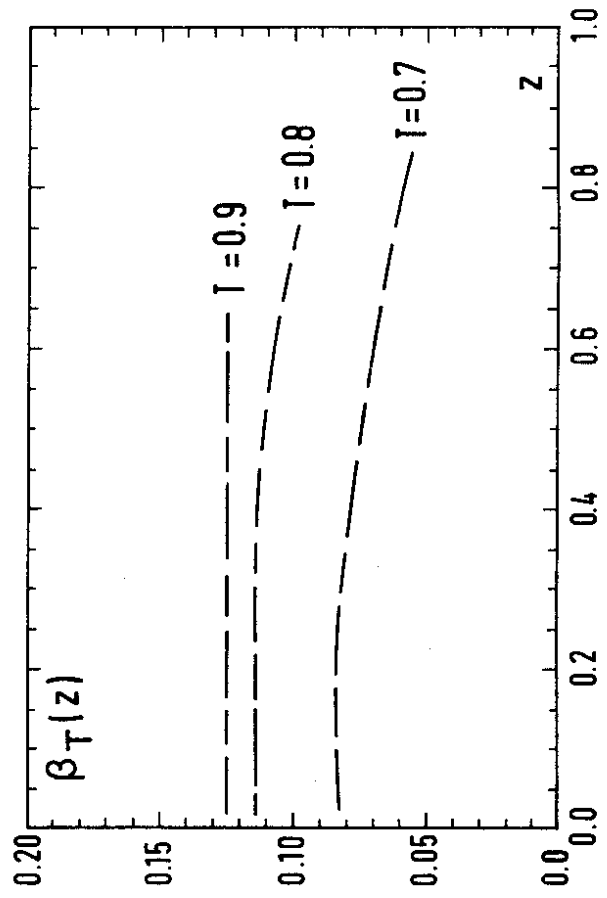


Fig. 5b

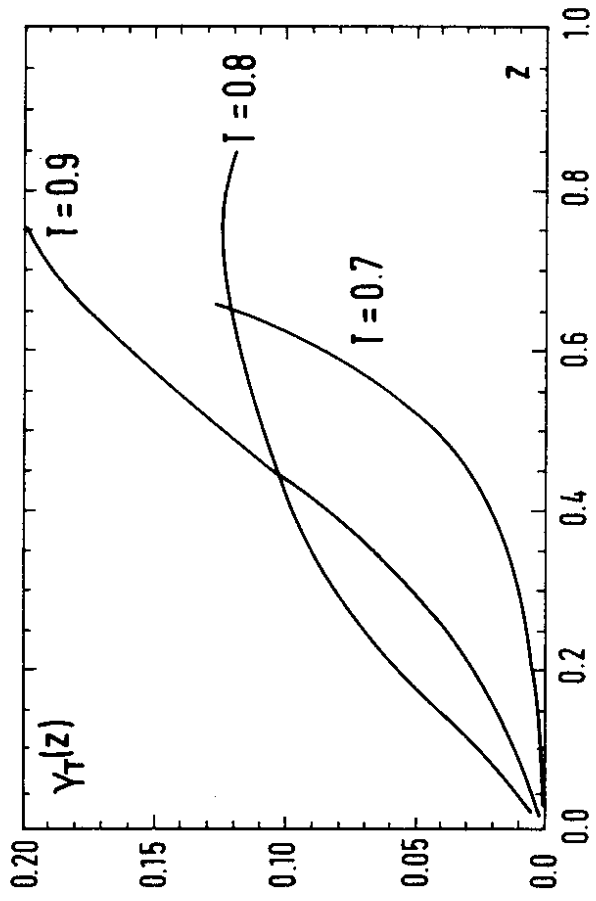


Fig. 6a

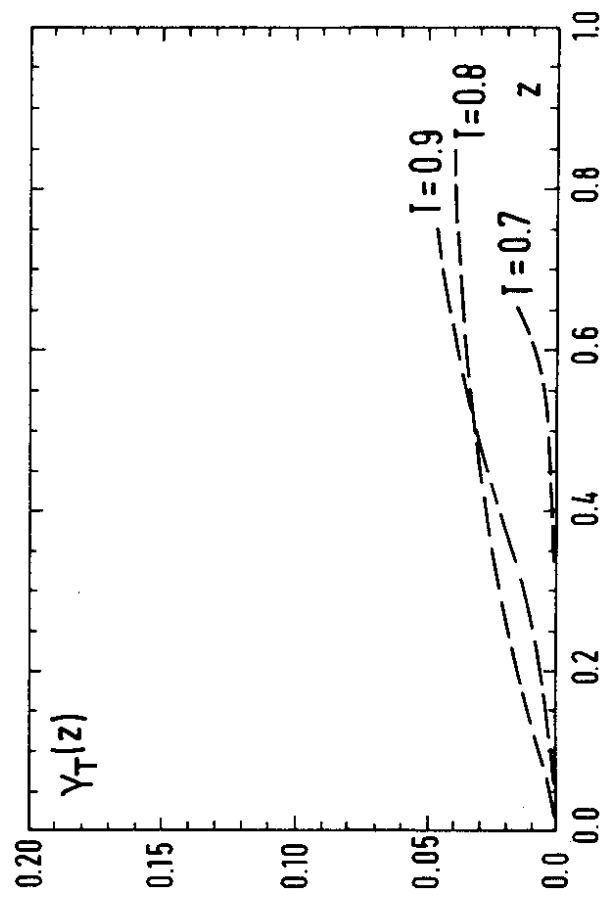


Fig. 6b